

# Highlights of the CMS Experiment



15<sup>th</sup> FCPPN/L Workshop, Bordeaux, France

11-June-2024

**Jie Xiao** *IP2I-Lyon*

*On-behalf of the CMS collaboration*



## CMS Detector performance

## Recent CMS Analyses

- ❖ Top sector: Entanglement in top quark pairs
- ❖ Higgs sector: Higgs produced in association with  $b$ -quarks
- ❖ Standard Model measurements
  - ❖ Event Shapes in Minimum Bias Events
  - ❖ Effective weak mixing angle
- ❖ Beyond SM searches
  - ❖  $Z' \rightarrow \tau\tau$  searches
  - ❖ Excited tau lepton in the  $\tau\tau\gamma$  final state
  - ❖ Search for Kaluza–Klein (KK) gluon resonances  $g_{KK}$
- ❖ SUSY searches: Stealth/R-parity violation (RPV) Stop Search

## Summary

CMS Detector performance

Recent CMS A

- ❖ Top sector: Ent
- ❖ Higgs sector: H
- ❖ Standard Mod
- ❖ Event Shape
- ❖ Effective wea
- ❖ Beyond SM se
- ❖  $Z' \rightarrow \tau\tau$  search
- ❖ Excited tau le
- ❖ Search for Ka
- ❖ SUSY searches
- ❖ B hadron phys

## Disclaimer

A lot of interesting analyses are not covered

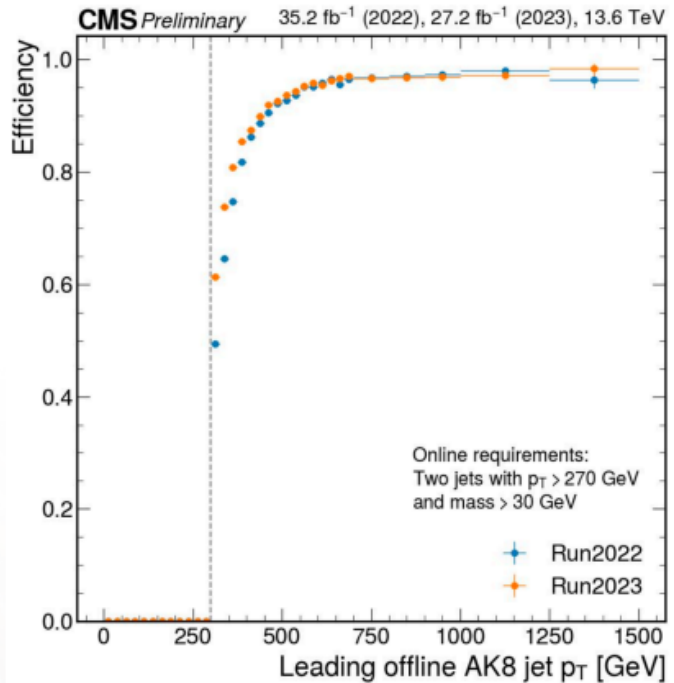
- ❖  $(X \rightarrow) HY/HH \rightarrow \gamma\gamma\tau\tau$  [CMS-PAS-HIG-22-012](#)
- ❖  $\gamma\gamma \rightarrow \tau\tau$  in pp and limits on  $\tau g-2$  [CMS-PAS-SMP-23-005](#)
- ❖ New structures in the  $J/\psi J/\psi$  spectrum [CMS-PAS-BPH-21-003](#), see the talk from [Kai](#)
- ❖ Run3 measurements
  - ❖ WW cross section measurement [CMS-PAS-SMP-24-001](#)
  - ❖ tW cross section measurement [CMS-PAS-TOP-23-008](#)
- ❖ Heavy ion studies
  - ❖ Double- $J/\psi$  meson production in pPb [CMS-PAS-HIN-23-013](#)
  - ❖ Azimuthal dependence of hyperon polarization [CMS-PAS-HIN-24-002](#)
  - ❖ Multiplicity dependence of  $\sigma_{\psi(2S)}/\sigma_{J/\psi}$  in pPb [CMS-PAS-HIN-24-001](#)
- ❖ Nice review papers
  - ❖ Physics of Dark Sectors in CMS [CMS-EXO-23-005](#)
  - ❖ Review of HY searches [CMS-B2G-23-002](#), see the talks from [Elise](#), [Chu](#)
- ❖ ...

Summary

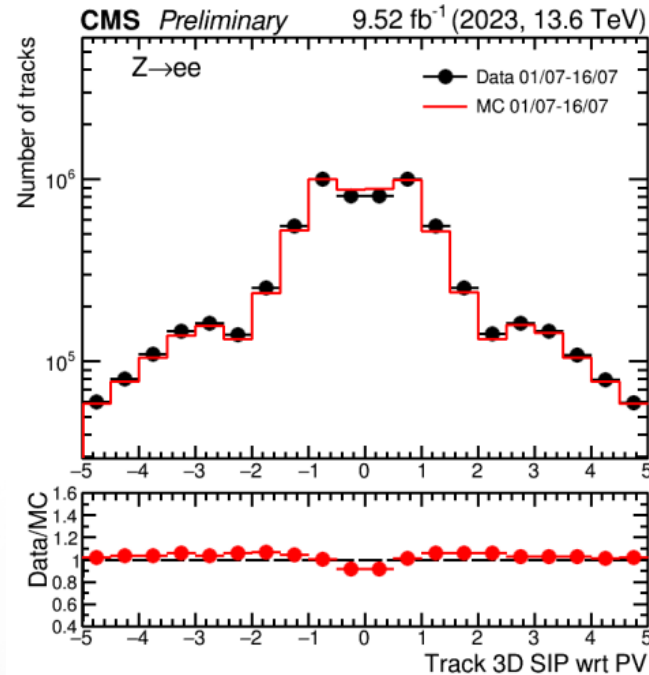
# Detector performance in Run 3



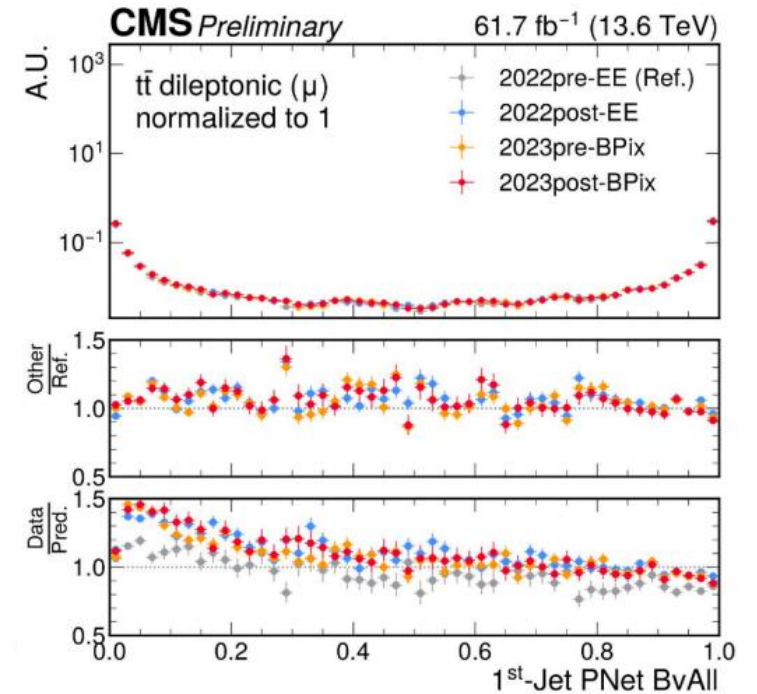
Stable and excellent performance



[CMS-DP-2023-094](#)  
Stability of HLT jet mass selection in Run 3

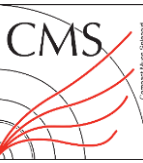


[CMS-DP-2023-090](#)  
Excellent performance of impact parameter significance in 3D for electron tracks in data and simulation



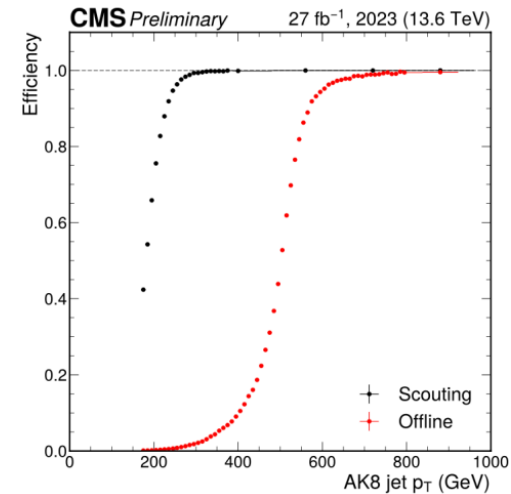
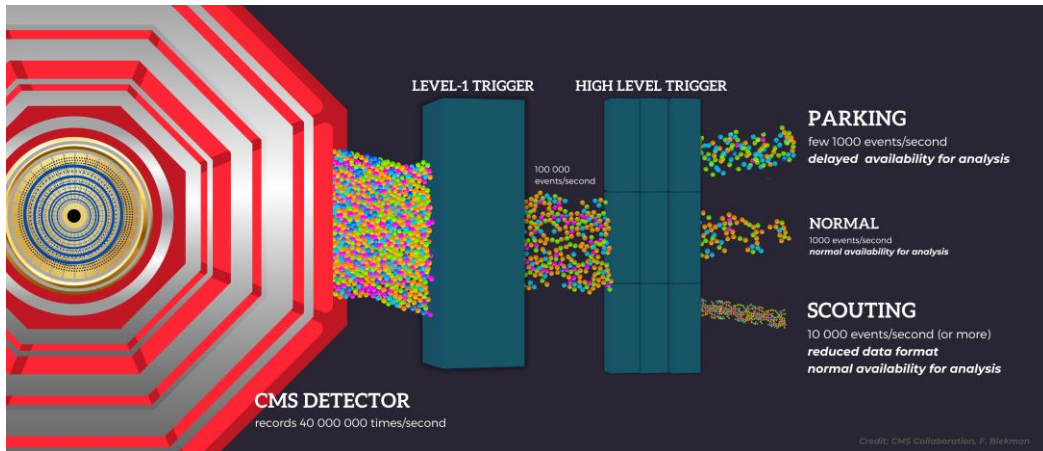
[CMS-DP-2024-024](#)  
Stable ParticleNet b-tag scores w.r.t. years and data taking periods

# From detector performance to physics potential



## Trigger strategies for Run3

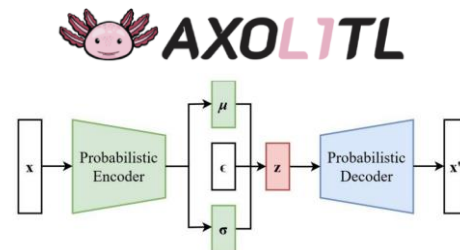
- ❖ Complementary approaches to support all physics cases within available resources
- ❖ Continuous development: new systems at L1 and improved GPU use at the HLT



[CMS-DP-2023-076](#)  
Lower threshold for  
largeradius jets with scouting

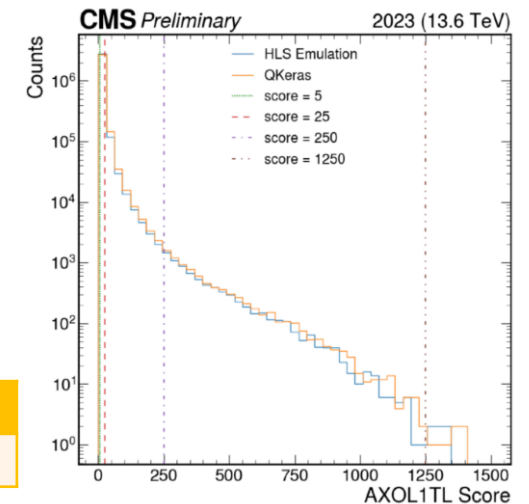
## Anomaly detection at L1

- ❖ E.g., **AXOL1TL**: variational auto encoder using input objects to global L1

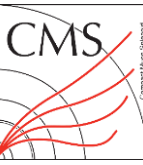


[CMS-DP-2023-079](#)  
AXOL1TL scores and efficiency  
gains vs standard L1 menu.  
Signal:  $H \rightarrow XX(15\text{GeV}) \rightarrow bbbb$

AXOL1TL Rate	1 kHz	5 kHz	10 kHz
Signal Efficiency Gain	46%	100%	133%



# Observation of top quark entanglement



Measure entanglement of top quark pairs in **dilepton** events using spin correlations

What does it mean to be entangled? Non-separable!

- ❖ To probe entanglement: Peres-Horodecki Criterion [[PRL.77.1413](#), [PLA232 \(1997\) 333](#)]
  - ❖ Hard to show it is separable but "easily" to show it is non-separable

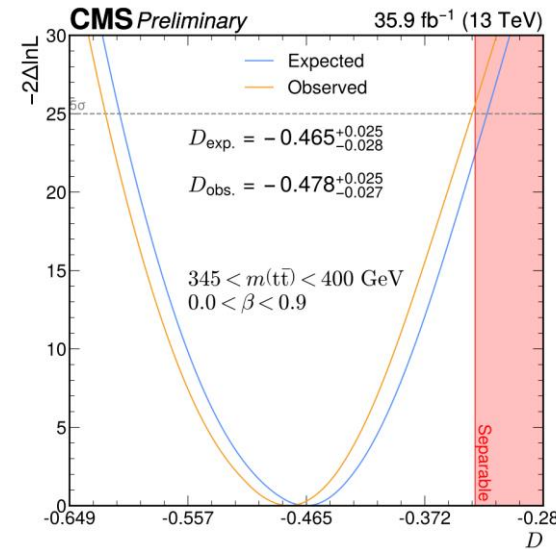
After some messy algebra a sufficient condition for entanglement is reached [[EPJP \(2021\) 136:907](#)]:

- ❖ Using diagonal elements:  $\Delta_E = -C_{33} + |C_{11} + C_{22}| > 1$
- ❖ Entanglement proxy  $D = \text{Tr}[C]/3$  (for small  $m_{t\bar{t}}$ ) can be extracted from angle between decay products

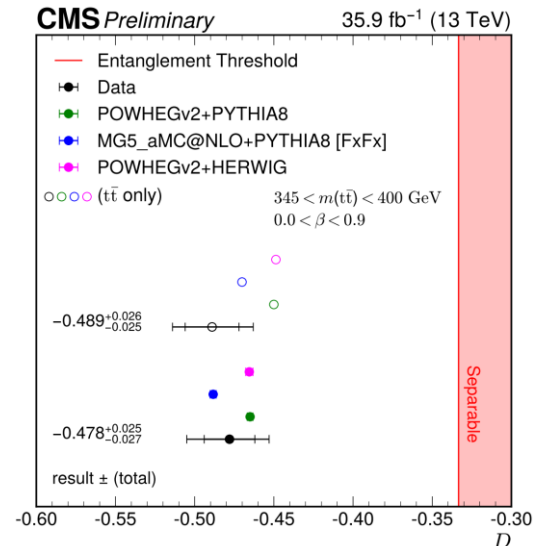
**Measure D to access entanglement information!**

$$\Delta \equiv -C_{33} + |C_{11} + C_{22}| - 1 > 0 \longrightarrow -\text{tr}[C] > 1 \longrightarrow D < -1/3$$

- ❖  $D < -1/3 \rightarrow$  **Entangled!**



$D < -1/3$  established at the  $5\sigma$  level

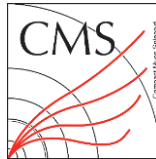


Higher sensitivity in the low  $m_{t\bar{t}}$  region

CMS-PAS-TOP-23-001

\* Atlas also observed the  $t\bar{t}$  entanglement [TOPQ-2021-24](#)

# Entanglement of top quark pairs via lepton+jets



## Measuring the correlation matrix in **single-leptonic** tt events

- ❖ All coefficients of polarization vectors and correlation matrix from fit to the angles of two decay products
  - ❖ Using NN to reconstruct the tt system in each event
- ❖ Test variables:
  - ❖  $\Delta_E$  from the full matrix:  $\Delta_E = C_{nn} + |C_{rr} + C_{kk}| > 1$
  - ❖ Two proxies  $D$  (for low  $m_{tt}$ ),  $\tilde{D}$  (for high  $m_{tt}$ )

**$D$  measurement**

Criterion for entanglement:  $D < -1/3$

$$D = \frac{1}{3}(C_{nn} + C_{rr} + C_{kk})$$

Spin-singlet state

**$\tilde{D}$  measurement**

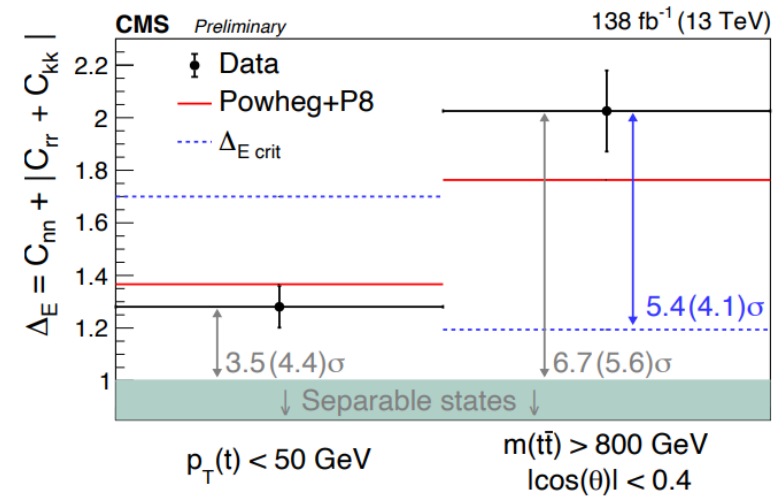
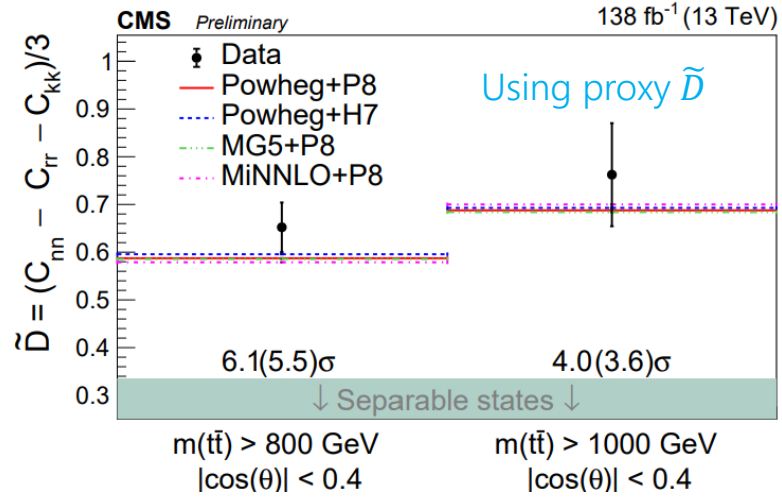
Criterion for entanglement:  $\tilde{D} > 1/3$

$$\tilde{D} = \frac{1}{3}(C_{nn} - C_{rr} - C_{kk})$$

Spin-singlet state

Higher  $m_{tt}$  allows to search exceeding maximum entanglement achievable by classical exchange of information

- ❖ Fraction of events with space-like separation increases with  $m_{tt}$ 
  - ❖ >90% for  $m_{tt} > 800\text{GeV}$



Separation from entanglement limit reaches 6.7 $\sigma$  obs (5.6 $\sigma$  exp) using  $\Delta_E$

CMS-PAS-TOP-23-007

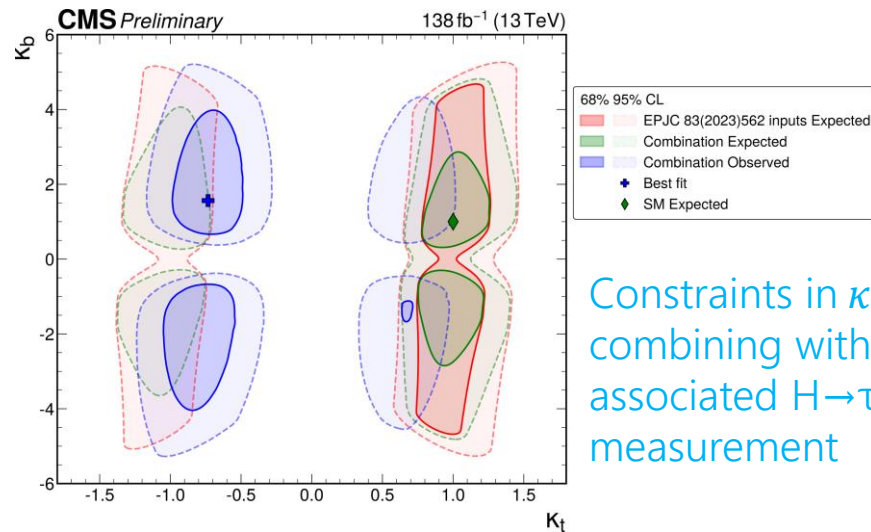
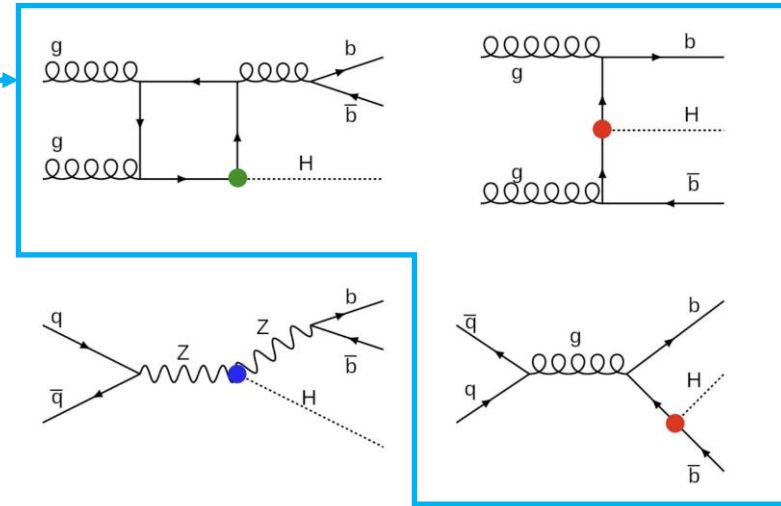
# Higgs produced in association with $b$ -quarks

Higgs production with associated  $b$ -quarks via

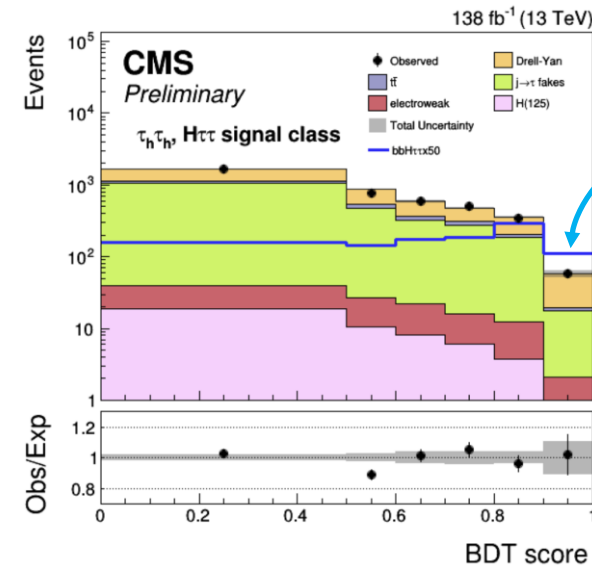
- ❖  $b$ -fusion
- ❖ gluon fusion with gluon  $\rightarrow$   $b\bar{b}$  splitting

Study the final states with leptons ( $WW, \tau\tau$ )

**Obs (exp) upper limit: 3.7 (6.1) x SM**

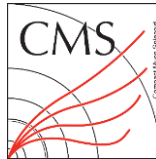


Constraints in  $\kappa_t, \kappa_b$  plane, combining with non  $b$ -associated  $H \rightarrow \tau\tau$  measurement





# Event Shapes in Minimum Bias Events

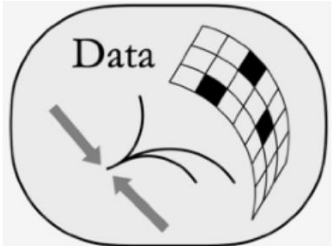


## Event shape observables

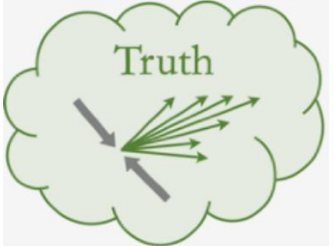
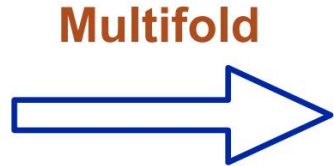
- ❖ Describing the “shapes” of the events  
→ Functions of the momentum of the final state particles
- ❖ An example: **transverse sphericity** →
- ❖ Others: (transverse) thrust, broadening, isotropy etc.

## Unfold with a machine-learning-based algorithm

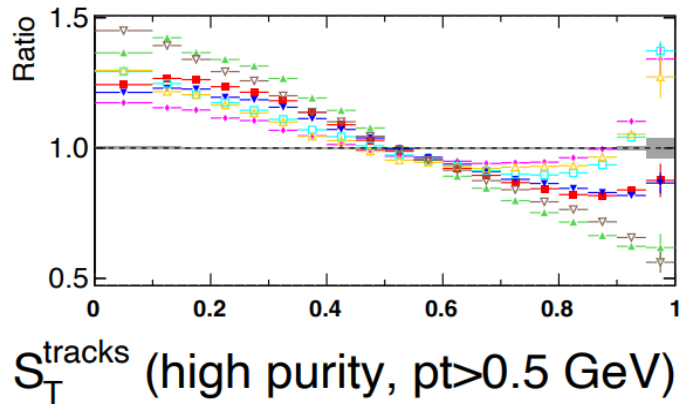
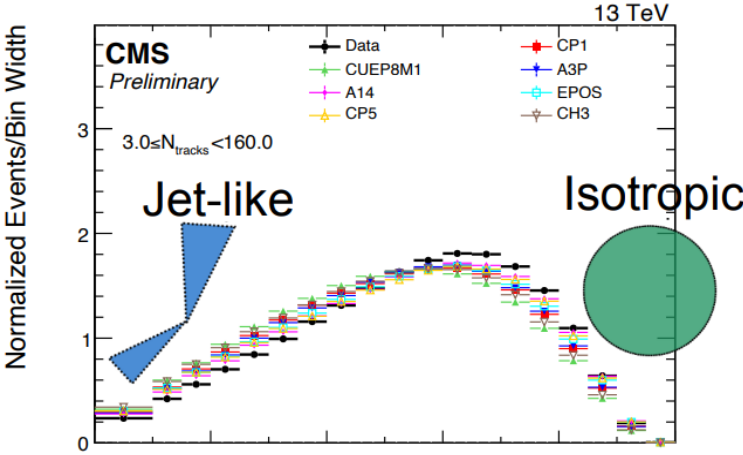
- ❖ Multifold\* [PRL.124.182001](https://arxiv.org/abs/1204.1820), [arXiv.2105.04448](https://arxiv.org/abs/2105.04448)



Event shapes of detector-level objects

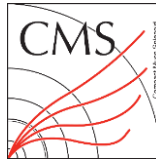


Event shapes of particles



CMS-PAS-SMP-23-008

# Event Shapes in Minimum Bias Events



Simultaneously unfold all the variables for ML-based weighting

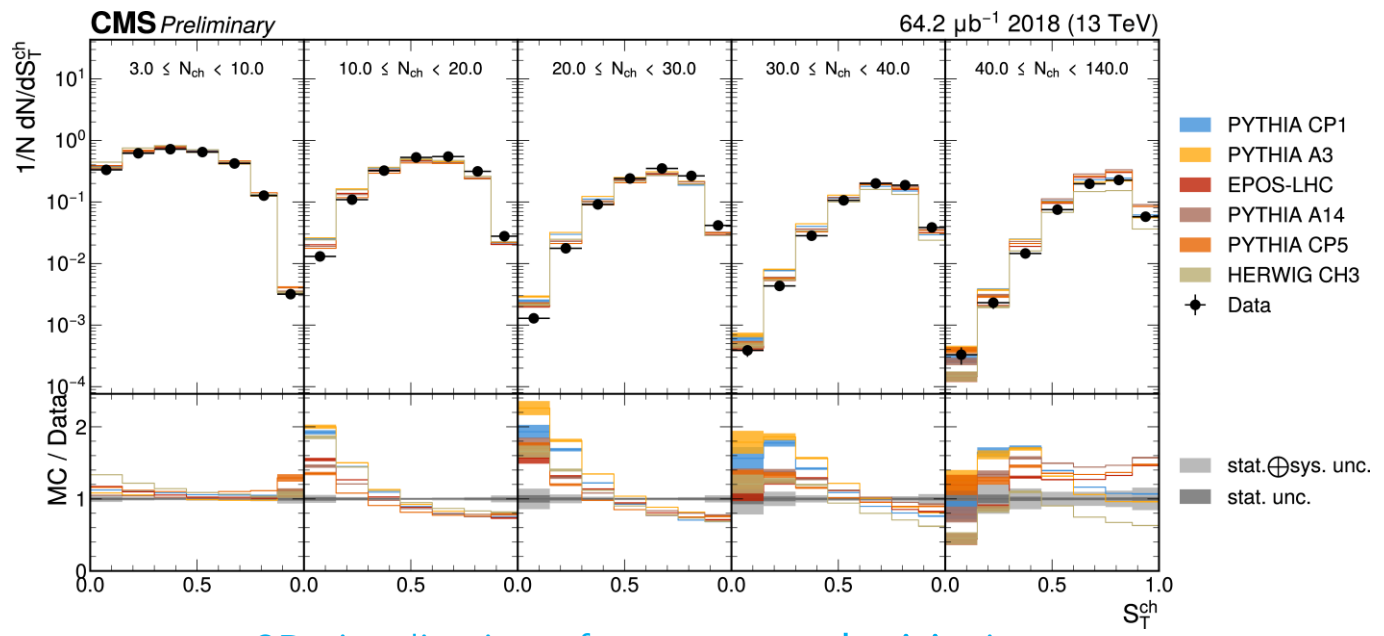
Add a variable to the unfolding:

- ❖ Methods based on binned histograms
  - ❖ Add another dimension in binning
  - ❖ Require higher statistics
  - ❖ More computations in simulation and unfolding
- ❖ ML-based method
  - ❖ Add a feature in the ML training and evaluation
  - ❖ Much easier to scale up the dimensions

More isotropic data than MC

- ❖ multi-parton-interaction model?
- ❖ collective effects?
- ❖ instantons?

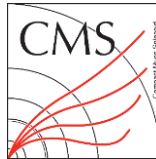
Provide the unfolded results for theoretical interpretation



2D visualization of transverse sphericity in charged particle multiplicity slices

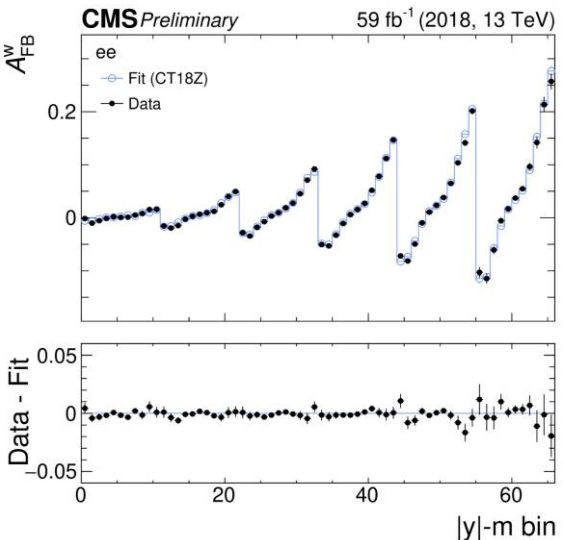
CMS-PAS-SMP-23-008

# Effective weak mixing angle



## Precision measurement of EWK key quantity at a hadron collider

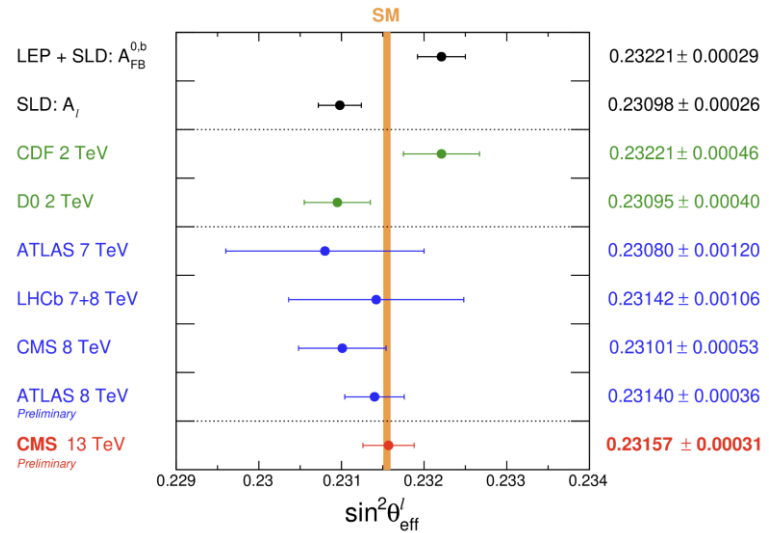
- ❖  $\sin^2 \theta_{\text{eff}}^l$  is extracted from simultaneous  $\chi^2$  fit of  $A_{FB}(y, m)$  in all di-muon or di-electron channels



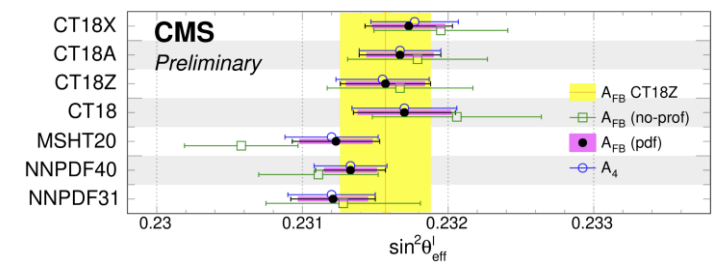
## Acceptance and sensitivity enhanced with extended acceptance for forward electrons

### ❖ Result (CT18Z)

$$\sin^2 \theta_{\text{eff}}^l = 0.23157 \pm 0.00010(\text{stat}) \pm 0.00015(\text{syst}) \pm 0.00009(\text{theo}) \pm 0.00027(\text{PDF})$$

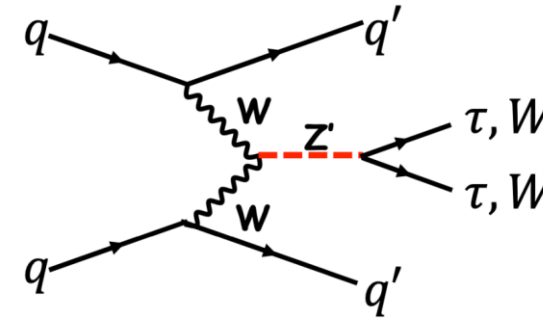
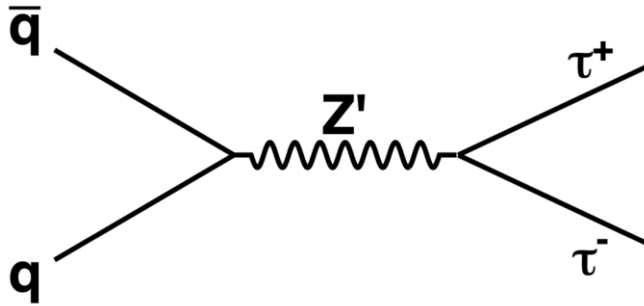


- ❖ Matches LEP/SLD precision
- ❖ Compatible with the SM prediction
- ❖ Adds to understanding of a long-standing tension between previous measurements



CMS-PAS-SMP-22-010

# Search for $Z'$ in $\tau\tau$ decay



Search in the  $e\tau_h$ ,  $\mu\tau_h$ , and  $\tau_h\tau_h$  final states

- ❖  $Z'$  not boosted  $\rightarrow$  high  $m_{Z'}$  two back-to-back  $\tau$

$$m_{Z'}^{reco} = \sqrt{(E_1^{\tau vis} + E_2^{\tau vis} + |p^{Z' miss}|)^2 - |p_1^{\tau vis} + p_2^{\tau vis} + p^{Z' miss}|^2}$$

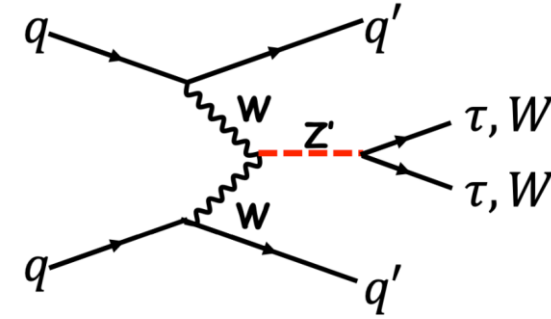
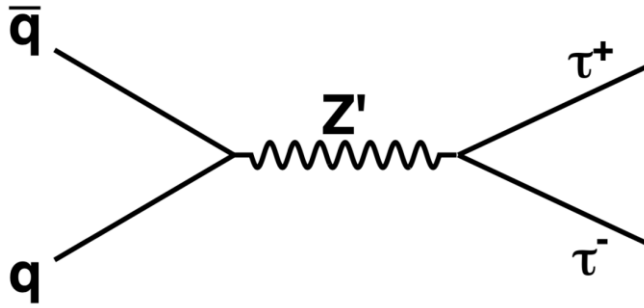
$$p^{Z' miss} = (-(\vec{p}_{1T}^{\tau vis} + \vec{p}_{2T}^{\tau vis}), 0)$$

Study the  $\tau\tau$  (the  $e\mu$ ,  $e\tau_h$ ,  $\mu\tau_h$ , and  $\tau_h\tau_h$  final states) and  $WW$  decays

- ❖ VBF topology requires a pair of well separated & in the opposite jets with high mass :
  - ❖  $|\Delta\eta_{jj}| > 4.2$  &  $|\eta_{j1}\eta_{j2}| < 0$
  - ❖  $m_{jj} > 500$  GeV
- ❖ Boost to the  $Z' \rightarrow p_T^{miss}$  from  $\tau$  decay is collinear with  $Z'$

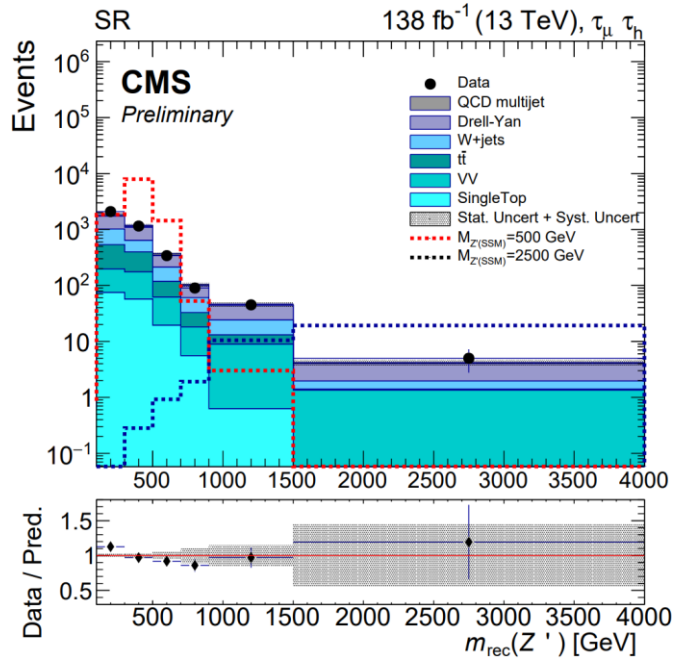
$$m_{Z'}^{reco} = \sqrt{(E_{e1} + E_{e2} + p_T^{miss})^2 - (\vec{p}_{e1} + \vec{p}_{e2} + \vec{p}_T^{miss})^2}$$

# Search for $Z'$ in $\tau\tau$ decay – backgrounds

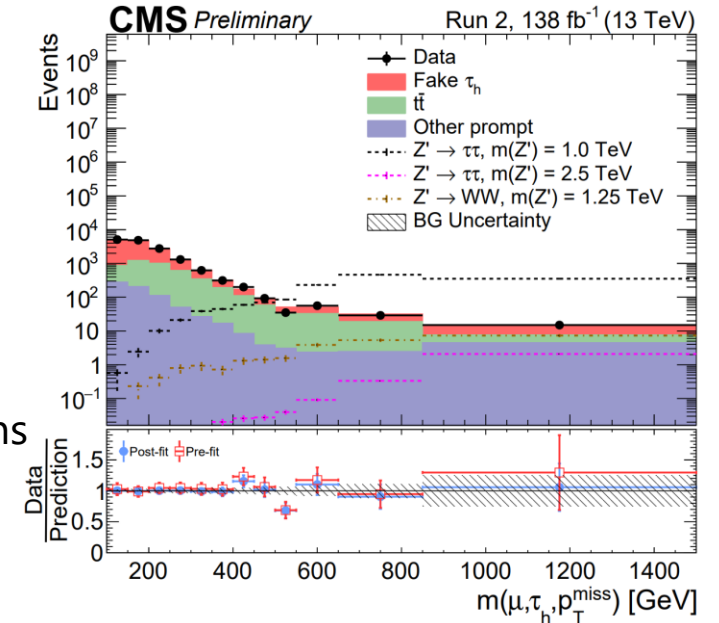


CMS-PAS-EXO-21-016

- ❖ QCD estimated with **ABCD** method
- ❖ Background estimation: DY, W, tt estimated by MC and normalizations from data

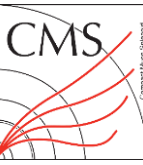


- ❖ Non-prompt: **loose-tight** method from sidebands
- ❖ Prompt bkg: estimated by MC and normalizations from data



CMS-PAS-EXO-21-015

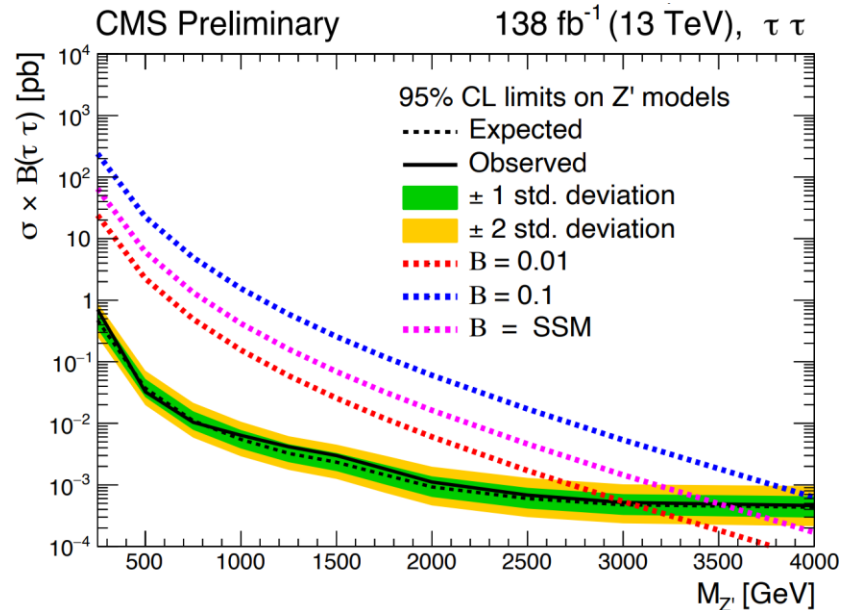
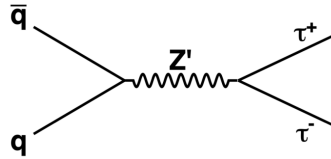
# Search for $Z'$ in $\tau\tau$ decay – results



Interpretation relies on Sequential Standard Model (SSM)

❖ Limits in mass range from **400 GeV to 4 TeV**

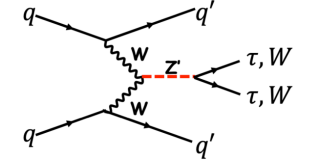
❖ **Most stringent limits for  $Z' \rightarrow \tau\tau$**



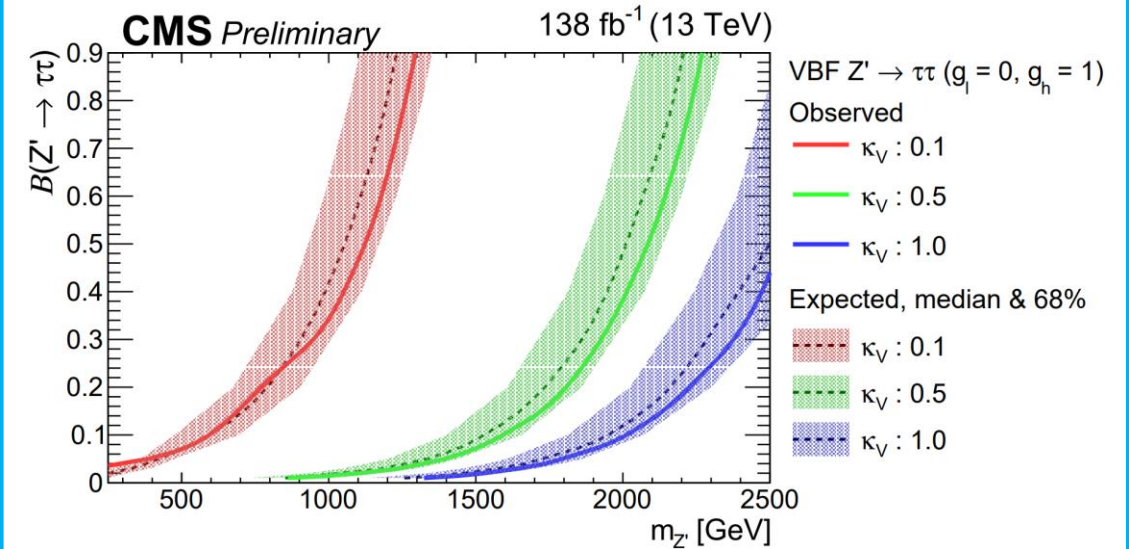
Interpretation relies on the SSM

❖ Four independent parameters:

- ❖  $Z'$  couplings to 1st+2nd ( $g_l$ ) and 3rd ( $g_h$ ) generations
- ❖ Coupling to  $W$  ( $\kappa_V$ )
- ❖  $Z'$  mass ( $m_{Z'}$ )



❖ **First interpretations of VBF produced  $Z'$  at the LHC**



CMS-PAS-EXO-21-016

CMS-PAS-EXO-21-015

# Excited tau lepton ( $\tau^*$ ) in the $\tau\tau\gamma$ final state

Excited states of the  $\tau$  would give evidence of compositeness

Contact interaction (CI) model predicts a  $\tau\tau + \text{high-}p_T \gamma$  final state

- ❖ Single excited  $\tau$  lepton ( $\tau^*$ ) is produced via a contact interaction (CI)

- ❖ CI production  $\rightarrow \mathcal{L}_{CI} = \frac{g^{*2}}{2\Lambda^2} j^\mu j_\mu$

- ❖  $\tau^*$  decays via emission of a SM photon

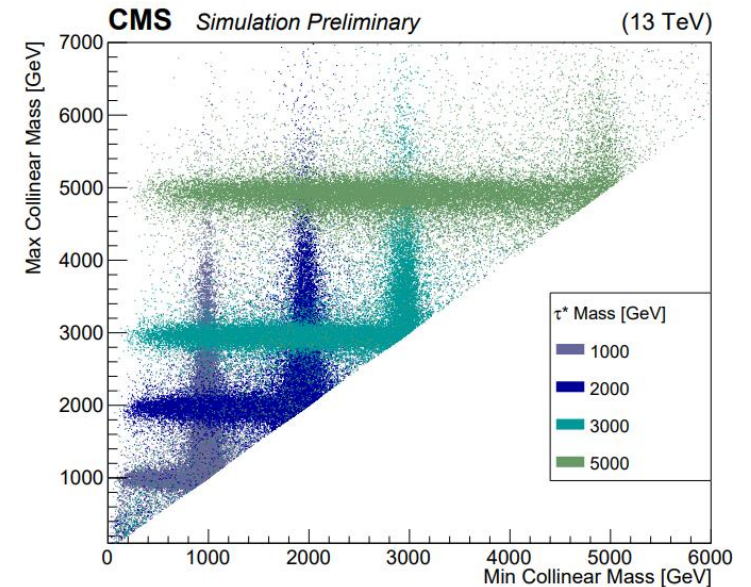
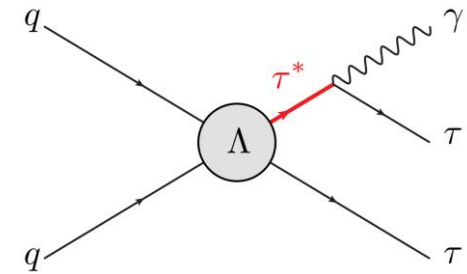
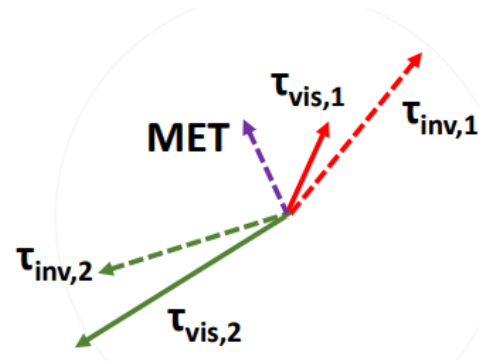
- ❖ SU(2) like decay  $\rightarrow \mathcal{L}_{GM} = \frac{1}{2\Lambda} \bar{f}_R^* \sigma^{\mu\nu} \left[ g f \frac{\tau}{2} W_{\mu\nu} + g' f' \frac{Y}{2} B_{\mu\nu} \right] f_L + h.c.$

Several steps to reconstruct the mass of the  $\tau^*$  in  $e\tau_h$ ,  $\mu\tau_h$ , and  $\tau_h\tau_h$

- ❖ Collinear approximation:

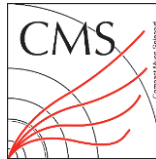
- ❖ Assume that  $\nu_\tau$  is collinear with the visible part of the  $\tau$  decay (either of  $\tau_h$ ,  $e$ ,  $\mu$ )

- ❖ Split  $p_T^{\text{miss}}$  into components from each  $\tau$



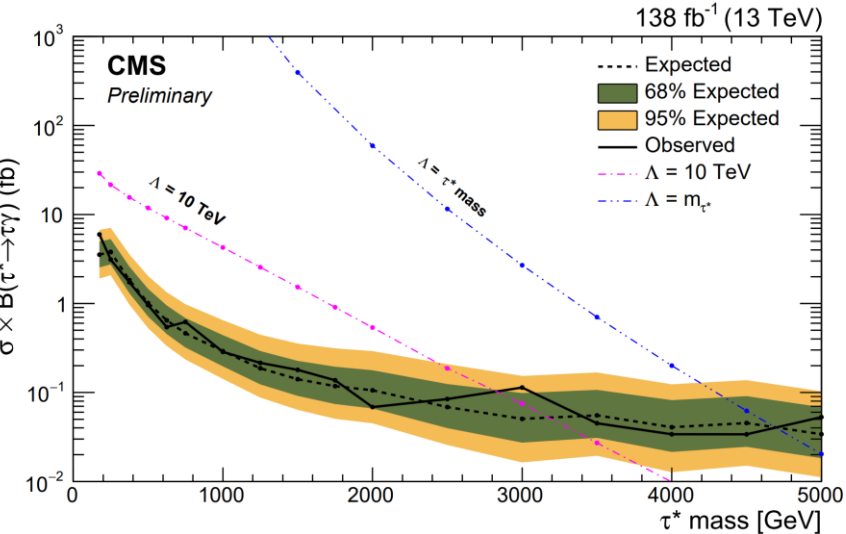
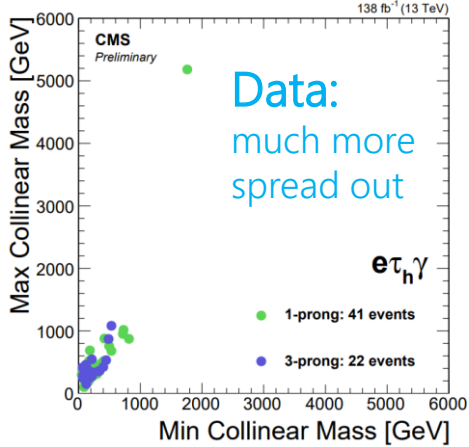
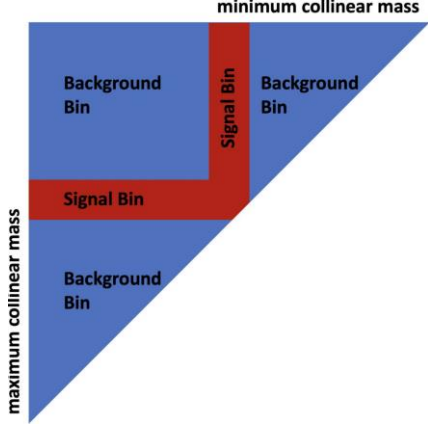
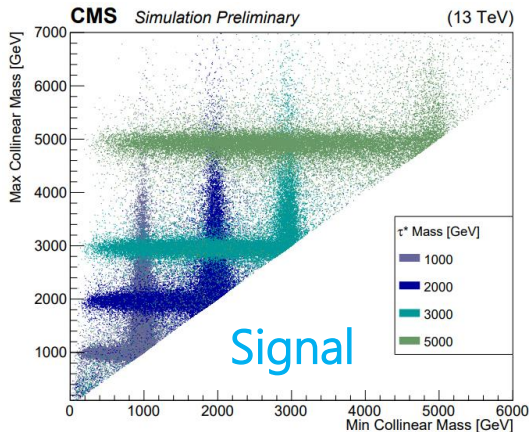
Signal populates a region in which either mass is compatible with  $m_{\tau^*}$

# Excited tau lepton ( $\tau^*$ ) in the $\tau\tau\gamma$ final state



The peculiarity of the L shape is used to define a parametric SR selection:

- ❖ Same data is used for all signal interpretations, but binning depends on the  $m_{\tau^*}$  hypothesis being tested



Depending on the assumptions on the CI energy scale:

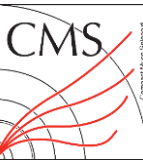
$\Lambda = 10 \text{ TeV} (m_{\tau^*}) \rightarrow$  **excluding  $m_{\tau^*} > 2.8 (4.7) \text{ TeV}$**

- ❖ Similar performance to the results obtained by ATLAS with a different strategy based on  $\tau\tau j j$  [JHEP 06 \(2023\) 199](#)

CMS-PAS-EXO-22-007

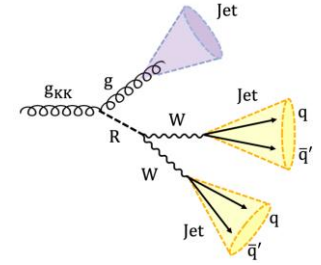


# Search for Kaluza–Klein (KK) gluon resonances $g_{KK}$



Cascade decay of  $g_{KK}$  into two  $W$  bosons and a gluon via a scalar radion  $R$

❖  $g_{KK} \rightarrow gR \rightarrow gW(qq)W(qq)$ : final state with three large-radius jets



Probing extended warped-extra-dimensional (WED) model

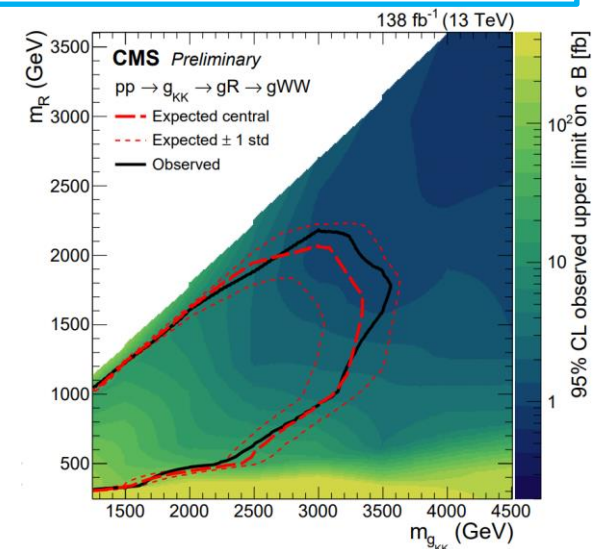
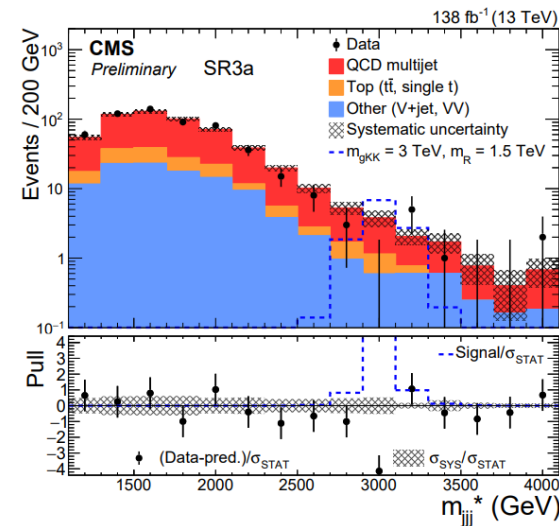
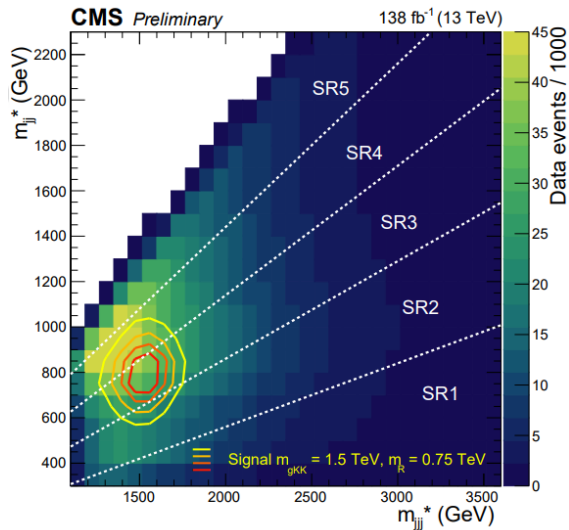
❖ With suppressed direct  $g_{KK}$  decay to SM particles

5 SRs defined in  $m(g_{KK})/m(R)$  plane

❖ Split further in two according to sub-leading  $W$  jet ParticleNet score

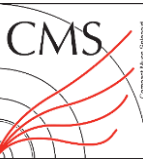
Limits on  $\sigma \times BR$  as a function of  $m(R)$  and  $m(g_{KK})$

- ❖ Excluding  $m(g_{KK})$  up to 3 TeV and  $m(R)$  up to 2.05 TeV for  $m(R) / m(g_{KK})$  in the range of 0.30–0.72
- ❖ Downward fluctuation of data at  $\sim 3$ –3.5 TeV  
Yield tight observed limits w.r.t. expectation



CMS-PAS-B2G-23-004

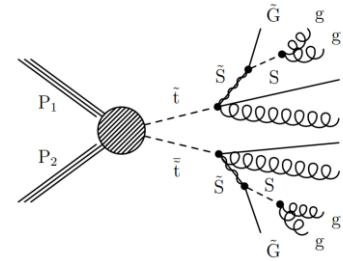
# Stealth/R-parity violation (RPV) Stop Search



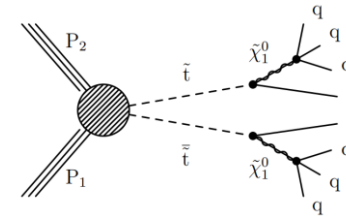
Looking for both an R-parity violating (RPV) and a Stealth SUSY Signature

- ❖ Final state: **ttbar+jets** with **little to no  $p_T^{\text{miss}}$**
- ❖ Primary observable is  $N_{\text{jets}}$
- ❖ Three channels: zero lepton (0l), one lepton (1l), and two lepton (2l)

Stealth  $S\bar{Y}\bar{Y}$  SUSY

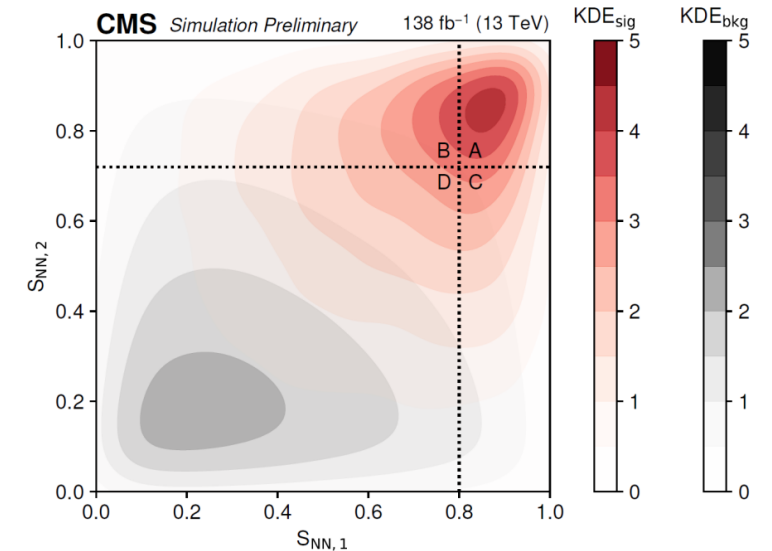


R-Parity Violating SUSY



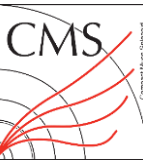
Signal and ttbar+jets estimated separately in each  $N_{\text{jets}}$  bin with simultaneous fit to data in four 'ABCD' bins of  $S_{\text{NN},1}$  vs.  $S_{\text{NN},2}$  plane

- ❖  $S_{\text{NN},1}$  and  $S_{\text{NN},2}$ : independent variables that discriminate signal from ttbar+jets generated using ABCDisCoTEC neural network (ML-based ABCD)
- ❖ Floating parameters of fit are ttbar+jets event yields in each ABCD bin and signal strength
- ❖ Fit relies on key 'ABCD' constraint:  $N_A = \kappa \frac{N_B N_C}{N_D}$ 
  - ❖ Appropriate given independence of  $S_{\text{NN},1}$  and  $S_{\text{NN},2}$



CMS-PAS-SUS-23-001

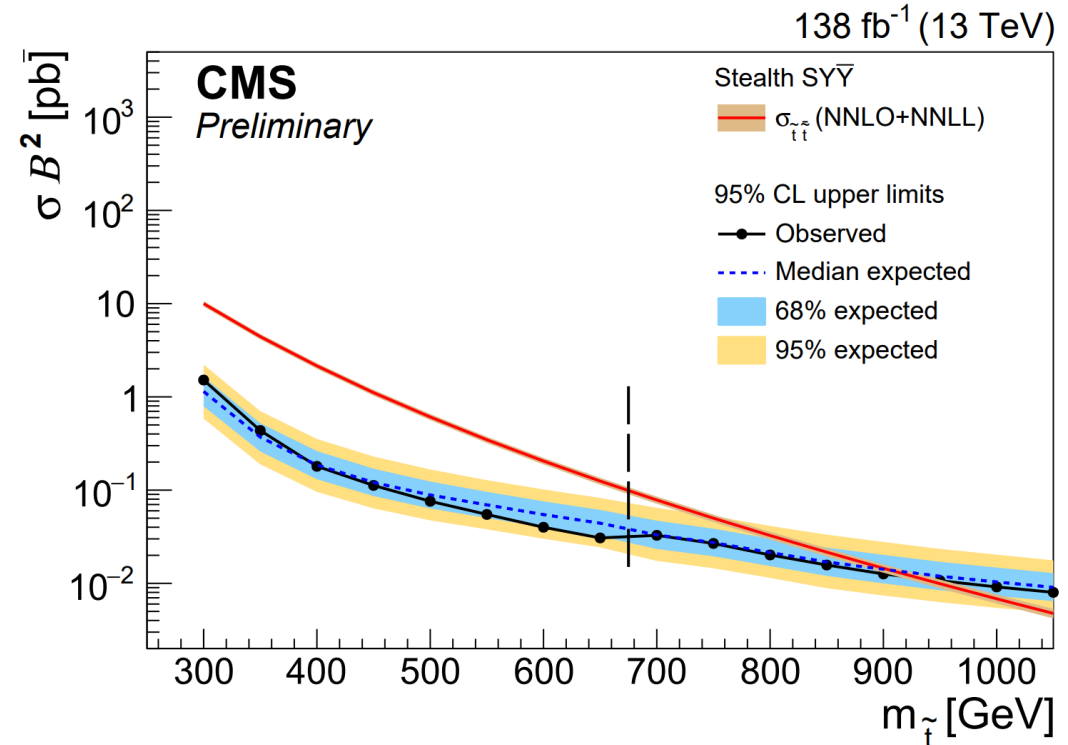
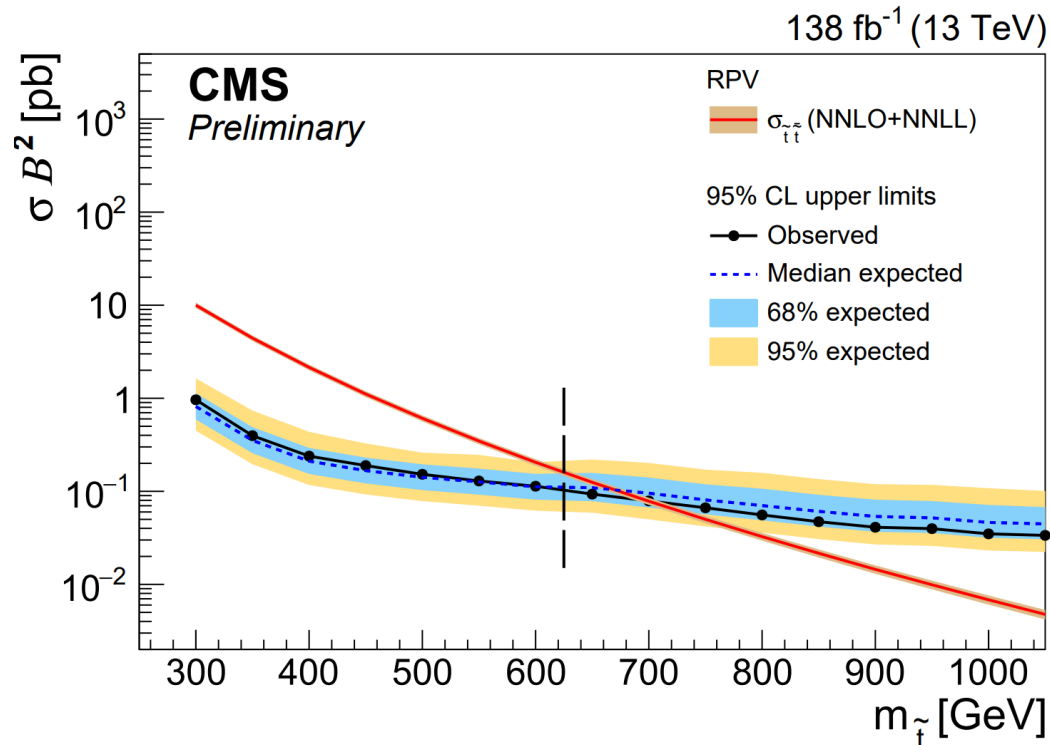
# Stealth/R-parity violation (RPV) Stop Search



Three channel combination limits shown for the RPV (left) and Stealth  $SY\bar{Y}$  (right) signal models

❖ No significant excess observed above expected background for either model

Mass exclusion limits set at 700 GeV (RPV) and 920 GeV (Stealth  $SY\bar{Y}$ )



# Summary



## Run 3 operations

- ❖ Stable and efficient data taking
- ❖ High quality of promptly reconstructed objects
- ❖ Trigger, data taking and reconstruction strategies open new possibilities for analysis

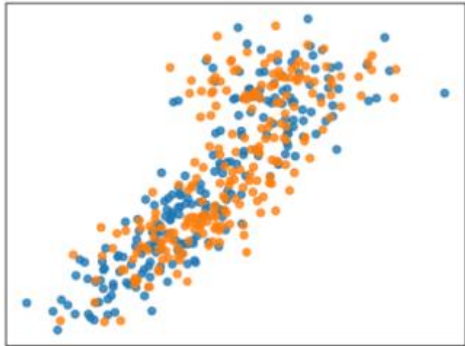
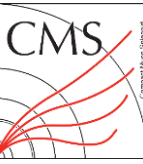
## Physics analysis: many new results since the winter conferences

- ❖ Entering the era of precision measurements
  - ❖ Some results on EWK physics now competitive with those from  $e^+e^-$
  - ❖ Investigating subtle effects as in  $t\bar{t}$  spin correlations
- ❖ Study of Higgs, BSM particles with multiple objects of
  - ❖ Tau leptons, top quarks, large radius jets, ...

# Backup

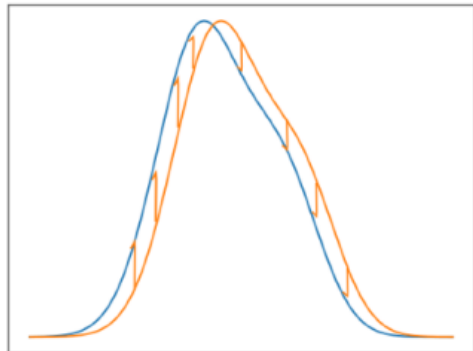
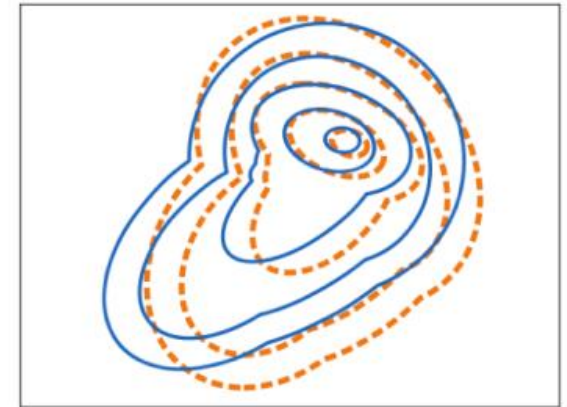


# Unbinned unfolding and uncertainty estimation



← A typical binary classifier to distinguish two sets

What it actually did: learn the differences in the distributions →



← Could use the classification scores to weight **MC** to **data**, and **nominal sample** to **systematic variations**

Event-wise unfolding → the result independent of binning

- ❖ Step 1: weight MC to data, at detector level
- ❖ Step 2: pull back the weights to particle(truth) level

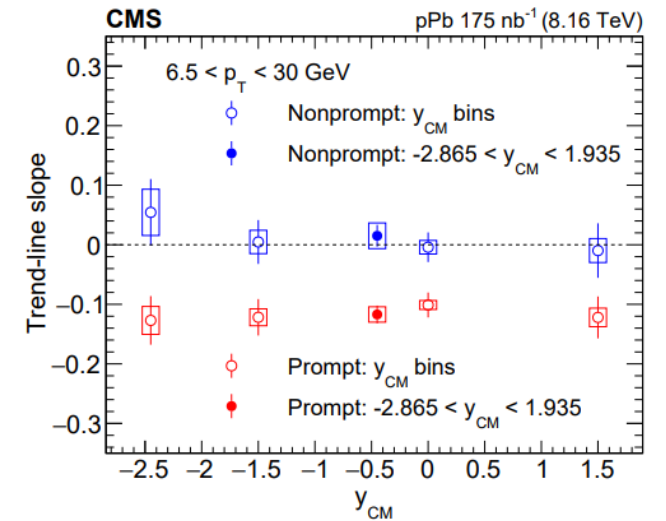
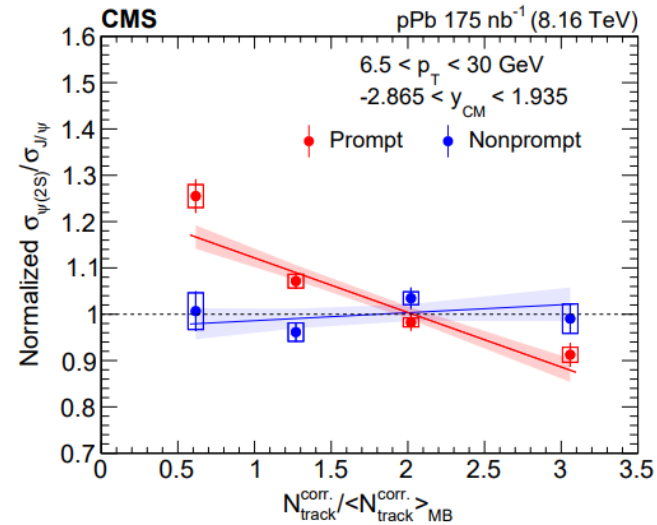
# Multiplicity dependence of $\sigma_{\psi(2S)}/\sigma_{J/\psi}$ in pPb

Ratio of  $\psi(2S)$  and  $J/\psi$  production cross sections in pPb collisions at  $\sqrt{s_{NN}} = 8.16\text{TeV}$

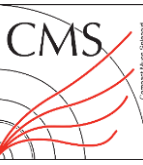
- ❖ Motivated by growing interest for quarkonium suppression in small systems
- ❖ Ratios measured for prompt and non-prompt mesons in the dimuon channel

Multiplicity-dependent modification of the ratio observed for prompt mesons

- ❖ Stable for non-prompt mesons
- ❖ Co-moving particles could dissociate excited states more easily than the ground state

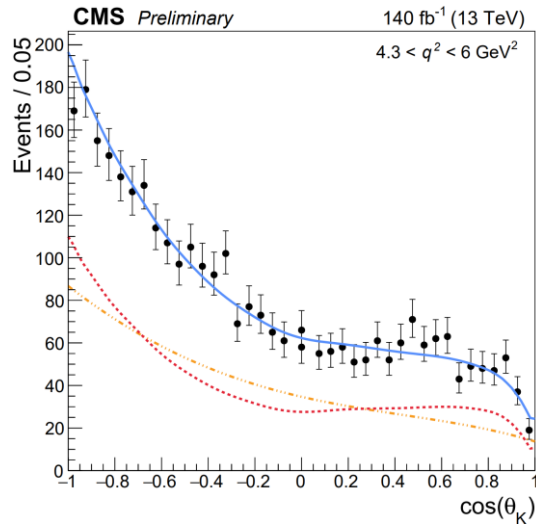
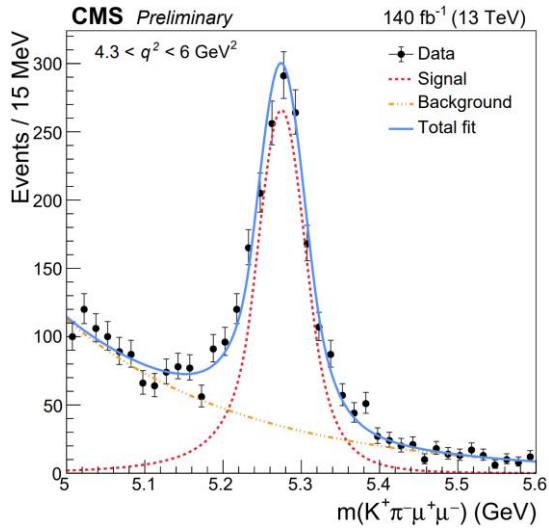
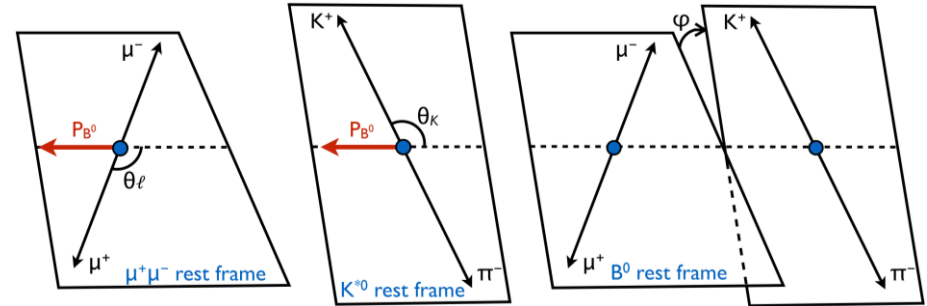


# Angular analysis of $B^0 \rightarrow K^{*0}(892)\mu^+\mu^-$



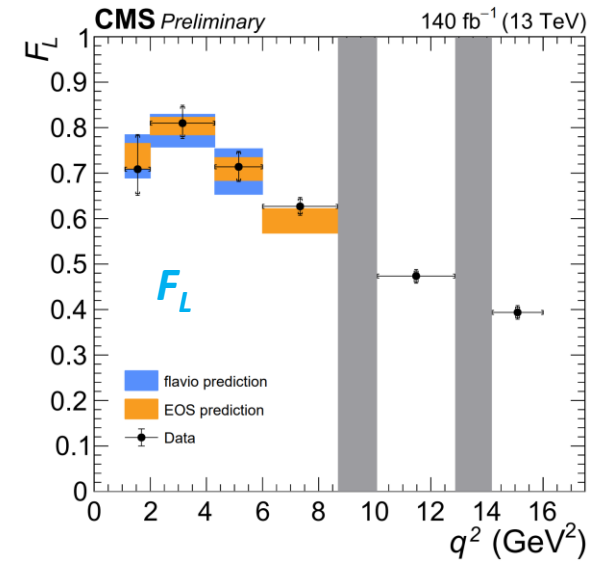
Measurement of the complete set of CP averaged variables

- ❖ Long history of searches for hints of new physics in this process
  - ❖ Limited impact of theoretical uncertainties in angular distributions
- ❖ Background rejection optimized with a BDT
- ❖ Angular parameters extracted from fit to  $m_B$  and 3 angles as  $f(q^2)$ 
  - ❖  $F_L, P_{1r}, P_{2r}, P_{3r}, P'_{4r}, P'_{5r}, P'_{6r}, P'_{8r}$



Post-fit mass and  $\cos(\theta_K)$  distributions

Results among the most precise measurements of these parameters



CMS-PAS-BPH-21-002